An approach to investigate the 3D height evolution in the crown crater during early crown formation with the General Defocusing Particle Tracking (GDPT) method

Pablo Molina Vogelsang*, Stefan Schubert, Grazia Lamanna
Institute of Aerospace Thermodynamics (ITLR), University of Stuttgart, Stuttgart, Germany
*Corresponding author: pablo.molina-vogelsang@itlr.uni-stuttgart.de

Introduction

The interaction between droplets and a wall film holds significance in various technical and natural-scientific processes, from raindrops impacting water puddles to industrial engine as a maintenance step. Analyzing the impact of a single drop on a thin liquid film reveals the radial growth of the crown crater and the simultaneous upward expansion of the crown wall. We focus our studies on the elevation phase, which describes the time between impact and maximum crown growth. Many phenomena such as the velocity field in the crown crater region or the 3D height evolution in the crown crater during early crown formation are not yet well understood. In the context of our research, we are developing a method to measure the 3D height evolution in the crown crater of early crown formation using the MATLAB code DefocusTracker (GDPT method) developed by Rossi and Barnkob [1][2]. Therefore, we presented a poster providing an overview of the experimental micro-PTV setup and the fundamentals of the evaluation routine (GDPT). Additionally, we showcased preliminary measurement results, illustrating how 3D information is obtained from a 2D image through the defocusing effect.

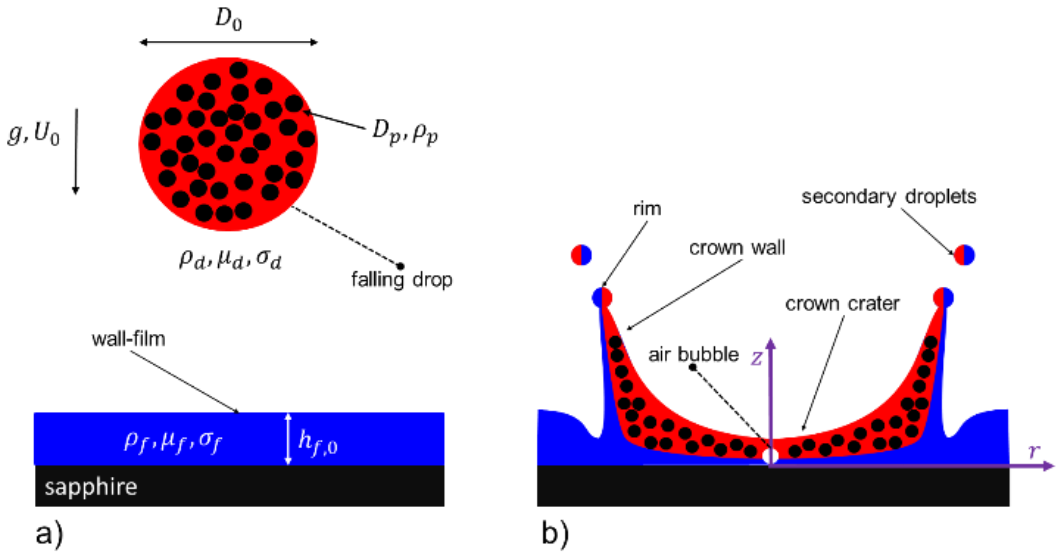

Figure 1. a) A single drop $(D_0, U_0, \rho_d, \mu_d, \sigma_d)$ seeded with tracer particles (D_p, ρ_p) falls onto a thin liquid film $(h_{f,0}, \rho_f, \mu_f, \sigma_f)$. b) The outcome: crown formation after the impact. The height evolution in the crown crater is defined by the ordinate z and the radially outward particle trajectories by the abscissa r.

Experimental setup and methods

The main components of the imaging system are an Axio Observer Z1 microscope from Carl Zeiss and two fully synchronized Photron Fastcam SA-X2 high-speed cameras: one for an oblique top view (macro view) and the other for a bottom view (micro view) through the microscope. The cameras are used to capture a series of 12-bit grayscale images with a resolution of 1024 x 1024 px² at a frame rate of 12,500 frames per second. Both views operate in backlight mode. We utilize a high-power LED for shadow graphics, with a color temperature of 6500 K for the oblique top view and 5000 K for the bottom view. Additionally, the experimental setup includes a droplet generation system (the droplet is seeded with Polystyrol trace particles), a light barrier (trigger) consisting of a 635-nm continuous wave laser with 1 mW power, and a pool. Figure 2 illustrates the experimental setup.

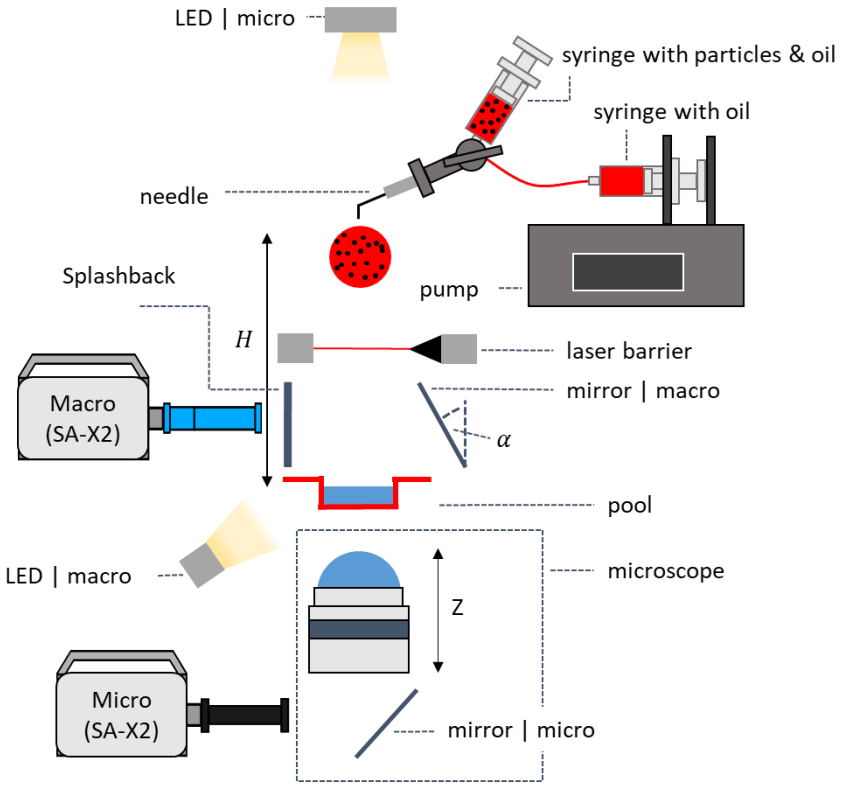

Figure 2. Schematic setup of the experimental facility for a given fall height H. It consists of the droplet generation system, the optical recording system and the impact area.

Defocusing is an optical principle that magnifies and blurs out-of-focus objects. This effect can be described using Newton's thin lens equation:

$$\frac{1}{f} = \frac{1}{S_O} + \frac{1}{S_i}. \tag{1}$$

where f the focal length, S_O the distance to the particle (object), and S_i the distance to the image ray intersection point is. Figure 3 illustrates the defocusing effect schematically. To illustrate this, two particles are considered: a red particle located at the height of the focal plane and a green particle located above the focal plane. Particles that are in the focal plane are in focus, while particles that are not on this plane appear larger and blurred. The optical effect of variations in particle size and scattering pattern (intensity) is used to obtain three-dimensional information (X, Y, Z) from a two-dimensional image (X, Y) with the use of defocusing technique.

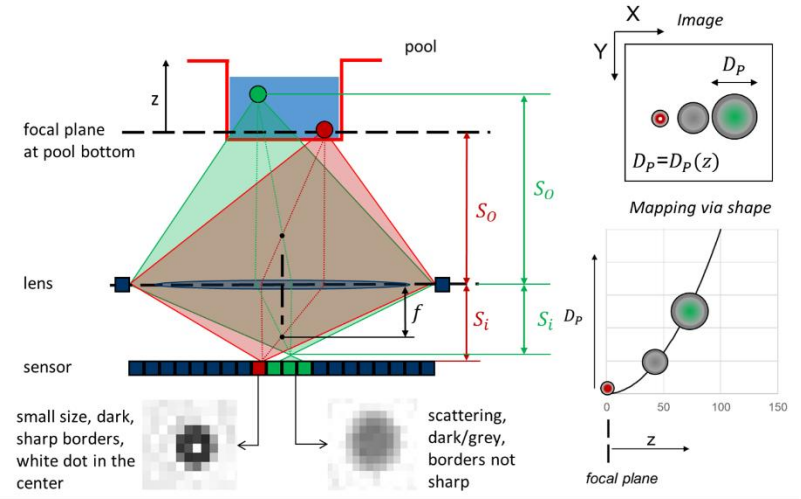

Figure 3. Schematic illustration of the optical principles of defocusing, with focal plane positioned at the pool bottom. This enables unique mapping of particles in 2D images (X, Y) based on shape and scattering, providing 3D (X, Y, Z) resolution. Additionally, having the focal plane at the pool bottom results in a reduction of the depth of field (DOF) by half. The green particles are located above the focal plane and occupy more sensors, while the red particles are in focus.

After the impact of the droplet in the pool, the formation of a crown crater is evident. By introducing particles into the droplet, the experimental µPTV setup enables the tracking of these particles in post-processing. The bottom view is used to determine the particle movement in the crown crater along (X,Y), while the defocusing technique provides insights into motion along Z.

The primary method for determining the depth position of the particles involves comparing the experimental images in post-processing with a set of reference images, called calibration stack. Therefore, a particle with higher density than the pool fluid is introduced. The particle sinks to the pool bottom and remains in a stationary state. Subsequently, the microscope is adjusted to predefined positions, causing a shift in the focal plane. This results in the appearance of the blurry and enlarged effect. During this process, images are captured. Figure 4 shows in simplified form what this process looks like.

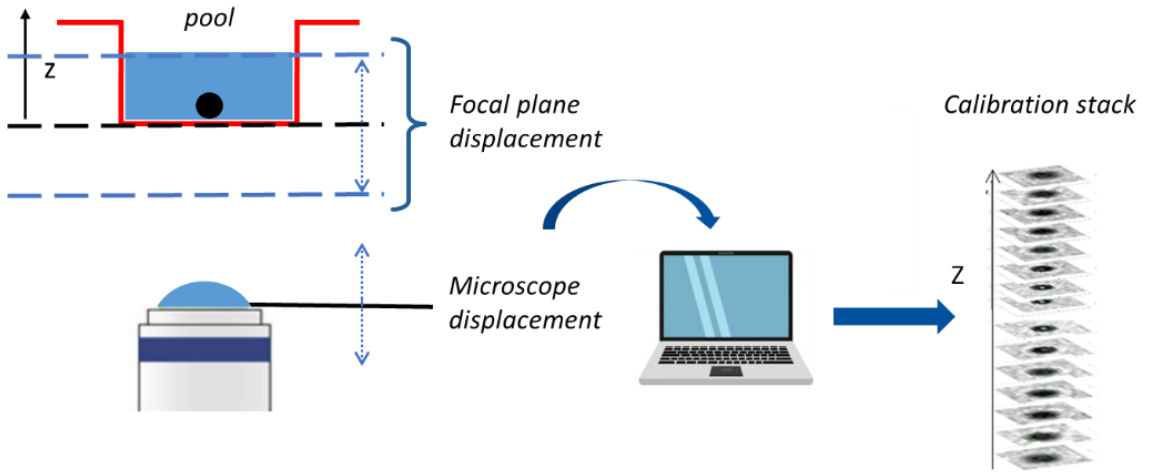

Figure 4. Creating a calibration stack - The microscope shifts its position to change the focal plane, resulting in blurry and enlarged particle images. At each predefined microscope step in z-axis, an image is captured.

The approach for investigating the 3D height evolution is divided into two sections. First, an calibration stack is created and then the 3D particle positions are reconstructed from the experimental images as part of the post-processing. In our measurement post-processing, we use the MATLAB code DefocusTracker based on the GDPT method. This method depends on the Normalized Cross-Correlation (NCC) algorithm, which relies on a user-defined Region of Interest (ROI). The primary aim of this approach is to assess the similarity between the ROI and the image with the correlation function $c(u,v)$: [3]

$$c(u,v) = \frac{\sum_{X,Y}[I_i(X,Y)-\bar{I}_i]\left[I_j(X-u,Y-v)-\bar{I}_j\right]}{\sqrt{\sum_{X,Y}[I_i(X,Y)-\bar{I}_i]^2 \sum_{X,Y}\left[I_j(X-u,Y-v)-\bar{I}_j\right]^2}}. \quad (2)$$

where $\bar{I}$ / I the averaged / Intensity, (u,v) the coordinates in the correlation space and (X,Y) the coordinates in the picture is. The maximization of similarity occurs when $u = v$. The maximum peak value of the correlation function is stored as the similarity coefficient $c_m(i,j)$. The range of c_m extends from 0 to 1, with 1 representing a perfect match, achieved when $i = j$, corresponding to the diagonal. A high-quality stack is characterized by significant differences in the generated images depending on Z, resulting in a variety of distinct c_m values.

Results and Discussion

To create a calibration stack, the pool was filled with a thin layer of silicone oil (B20) and a few particles made of polystyrol. Due to sedimentation, particles $\rho_p = 1050\ \frac{\mathrm{kg}}{\mathrm{m}^3} > \rho_f = 955\ \frac{\mathrm{kg}}{\mathrm{m}^3}$ sink to the bottom of the pool. The thickness of the thin layer $h_{f,0}$ was measured using the Confocal Chromatic Imaging (CCI) method and amounted to $h_{f,0} = 0.37\ \mu\mathrm{m}$. As the microscope was moved along the Z-axis, the focal plane was adjusted, and a photo was taken at each step with 2 µm step size.

Figure 5 displays two shadow images of the pool bottom. In the first image, where the focal plane is very close to the pool bottom, we define $z = z_1$, and in the last image with $z = z_2 = z_1 + \Delta z$. The original image of 1024 x 1024 px² was cropped for clarity to approximately 130 x 190 px². For evaluation, the second particle from the top was selected at $(X,Y) = (71\ \mathrm{px}, 43\ \mathrm{px})$. Images 1' and 2' depict the particle for z_1 and z_2 within the region of interest (ROI). In green, the particle detection is performed in post-processing using our MATLAB code based on Rossi's and Barnkob's [1][2] GDPT method. The defocusing effect is recognized with a diameter increasing from 6 to 8 pixels.

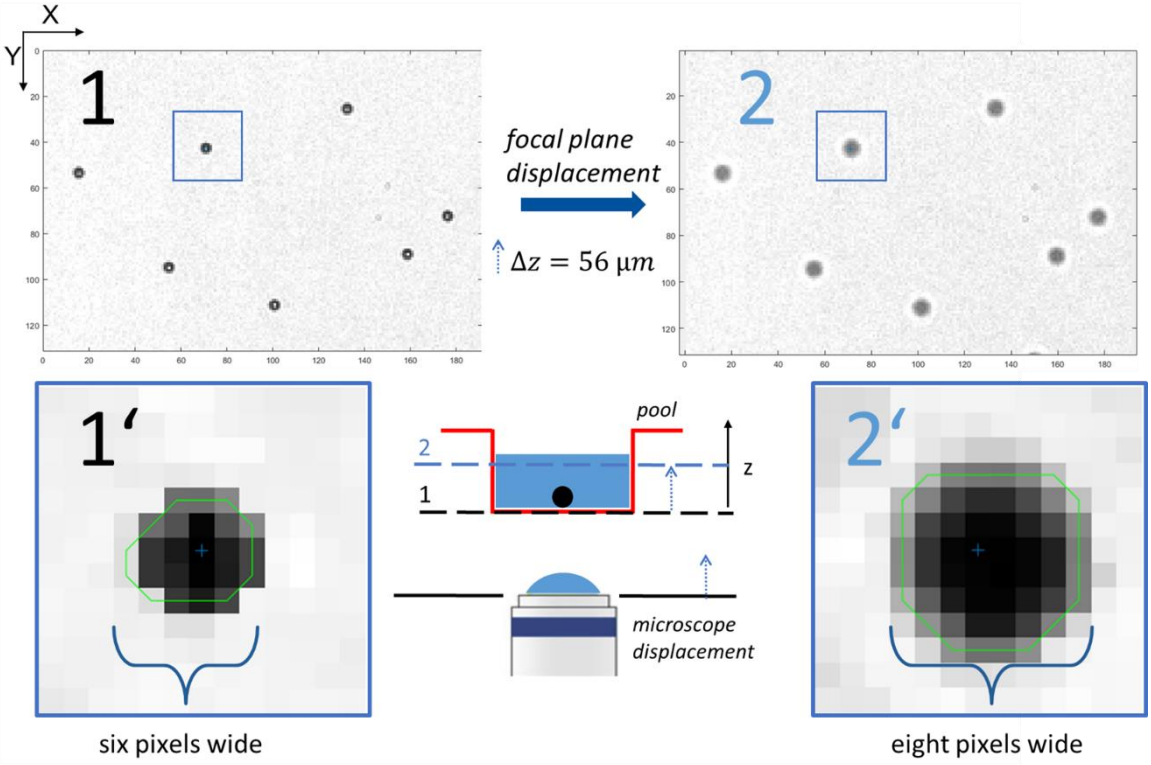

Figure 5. Pool bottom shadow images - Two shadow images of the pool bottom are presented. The first image, taken with the focal plane in close proximity to the pool bottom. The second image illustrates the defocusing effect at a microscope shift of $\Delta z = 56\ \mu m$. The particle size increases from 6 to 8 pixels.

In summary, the presented experimental setup allows for the generation of 2D data (X, Y) through the bottom view of the pool. The defocusing effect, leading to the blurring and enlargement of individual particles in the image, further enables the extraction of three-dimensional (3D) information (X, Y, Z). In the next step, we intend to investigate the impact of individual droplets on a thin liquid film from the bottom view. In this context, the GDPT method will also be applied. The information generated regarding the height (Z) of particles will then be matched with the calibration stack. Through this approach, we aim to gain insights into the 3D height evolution in the crown crater during early crown formation with the General Defocusing Particle Tracking (GDPT) method.

Nomenclature

D_0	Droplet diameter [m]
U_0	Impact velocity of a single drop [m s^-1]
$\rho_{d,f}$	Density of the trace particle ($_d$) or droplet fluid and wall-film ($_f$) [kg m^-3]
$\mu_{d,f}$	Dynamic of the trace particle ($_d$) or droplet fluid and wall-film ($_f$) [kg m^-1 s^-1]
$\sigma_{d,f}$	Surface tension of the trace particle ($_d$) or droplet fluid and wall-film ($_f$) [kg s^-2]
$h_{f,0}$	Height of the wall-film [m]
$\mathrm{X, Y, Z}$	Cartesian coordinates of a particle [m]
C_x, C_x	Coordinate of the impact center [m]
$\bar{I}$ / I	The averaged / Intensity [-]
f, S_0, S_i	Focal point, distance to the particle (object), distance to the image crossing point [m]

References

[1] M. Rossi, and R. Barnkob. A fast and robust algorithm for general defocusing particle tracking. Measurement Science and Technology. 32(1). (2021).
doi: https://dx.doi.org/10.1088/1361-6501/abad71
[2] R. Barnkob, and M. Rossi. DefocusTracker: A Modular Toolbox for Defocusing-based, Single-Camera, 3D Particle Tracking. Journal of Open Research Software. 9(1). (2021).
doi: http://doi.org/10.5334/jors.351
[3] Rune Barnkob and Massimiliano Rossi. General defocusing particle tracking: fundamentals and uncertainty assessment. Experiments in Fluids, 61(4), apr 2020. 7, 9, 18